ISSN 1070-3284, Russian Journal of Coordination Chemistry, 2023, Vol. 49, No. 4, pp. 218–229. © Pleiades Publishing, Ltd., 2023.
Russian Text © The Author(s), 2023, published in Koordinatsionnaya Khimiya, 2023, Vol. 49, No. 4, pp. 217–228.

Cationic Complexes of 3a,6a-Diaza-1,4-diphosphapentalenes

V. V. Sushev[a], Yu. S. Panova[a], A. V. Khristolyubova[a], N. V. Zolotareva[a], M. D. Grishin[a], E. V. Baranov[a], G. K. Fukin[a], and A. N. Kornev[a, *]

[a] *Razuvaev Institute of Organometallic Chemistry, Russian Academy of Sciences, Nizhny Novgorod, Russia*

**e-mail: akornev@iomc.ras.ru*

Received July 5, 2022; revised July 27, 2022; accepted August 2, 2022

Abstract—The reactions of annulated 1,4-dichloro-3a,6a-diaza-1,4-diphosphapentalenes ($DDPCl_2$) with 1 equiv. of trimethylsilyl triflate (TMSOTf) lead to replacement of one chlorine atom with the triflate group, thus giving cationic diazadiphosphapentalenes $[ClDDP]^+[TfO]^-$. In the presence of 2 equiv. of TMSOTf and 2 equiv. of 4-dimethylaminopyridine (DMAP), the DDP dication stabilized by two DMAP molecules, $[DDP(DMAP)_2]^{2+}[(CF_3SO_3)^-]_2$, is formed. The DMAP molecules are located on one side of the DDP skeleton and lie in parallel planes. Free diazadiphosphapentalene was detected in solutions of $[DDP(DMAP)_2]^{2+}[(CF_3SO_3)^-]_2$ in CH_2Cl_2 by UV-Vis spectroscopy and CV. This implies that this compound disproportionates under these conditions; it is unstable in dilute solutions and decomposes to give [DMAP·HOTf] in a quantitative yield. Crystallographic data for the obtained compounds: CCDC nos. 2182881–2182883.

Keywords: diazadiphosphapentalenes, diazaphospholes, two-coordinate phosphorus, phosphenium cations

DOI: 10.1134/S1070328423700458

INTRODUCTION

3a,6a-Diaza-1,4-diphosphapentalenes (DDPs) are a new class of organophosphorus heterocycles, which behave as latent phosphinidenes [1, 2]. The dual reactivity of DDPs is due to the change in the electron configuration of phosphorus under the action of polarizing factors, which are usually represented by metal ions or Lewis acids (Scheme 1) [3, 4].

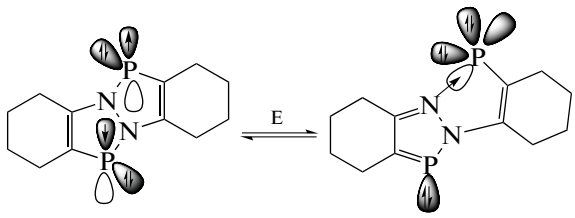

Scheme 1.

Owing to this electron density transfer towards one phosphorus atom, diazadiphosphapentalene can coordinate one (E = Ph_3B, InI_3, $[SbCl_4]^-$, $GeCl_2$, $HgCl_2$, Scheme 2A) [1, 3, 5] or two electrophilic centers (E = Ph_2BCl, Scheme 2B) [4]. When one electrophilic center is coordinated, it is located above the plane of the heterocycle.

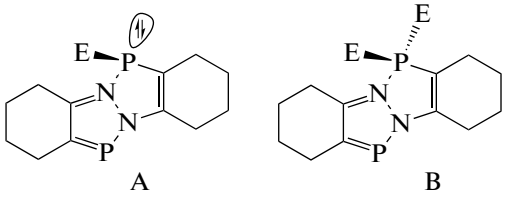

Scheme 2.

A versatile study of the coordination activity of diazadiphosphapentalenes showed that the phosphorus atoms in these heterocycles can not only function as donors of free electron pairs, but can also act themselves as electrophilic coordination sites at the deficiency of electron density.

This study addresses the reaction of DDP dichlorides with trimethylsilyl triflate, resulting in the cationic derivatives of diazadiphosphapentalenes, which may be stabilized by donor ligands.

EXPERIMENTAL

The syntheses were conducted in vacuum or in a high-purity argon atmosphere. Tetrahydrofuran (THF) was purified by refluxing over sodium in the presence of benzophenone (ketyl-Na). Dichloromethane and toluene were distilled from P_2O_5. Pyridine was refluxed over KOH and distilled. 4-Dimethylaminopyridine (DMAP) (≥99%, Sigma-Aldrich) and trimethylsilyl triflate ($Me_3SiOSO_2CF_3$, TMSOTf) (≥99%, Sigma-Aldrich) were used as received and stored in tubes under argon.

Synthesis of $[(DDP)(DMAP)_2](OTf)_2$ (II). Solutions of trimethylsilyl triflate (0.44 g, 2.0 mmol) and 4-dimethylaminopyridine (0.24 g, 2.0 mmol) in dichloromethane (10 mL each) were successively added at 0°C to a solution of cyclohexane-annulated 1,4-dichloro-3a,6a-diaza-1,4-diphosphapentalene (**I**, [6]) (0.32 g, 1.0 mmol) in dichloromethane (15 mL). The reaction mixture was kept for 1 h at room temperature and concentrated. The precipitated colorless

crystals were recrystallized from acetonitrile. The yield of **II** was 0.72 g (92%).

For $C_{28}H_{36}F_6N_6O_6P_2S_2$ (M = 792.69)

Anal. calcd., %	C, 42.43	H, 4.58	N, 10.60	P, 7.81
Found, %	C, 42.37	H, 4.63	N, 10.56	P, 7.84

^{1}H NMR ($CDCl_3$, δ, ppm): 7.80 (br.s., 4 H, Py); 6.95 (d. $^3J_{H,H}$ = 6 Hz, 4 H, Py), 3.25 (s, 12H, CH_3), 3.10–1.40 (m, 16 H, cHex). $^{31}P\{^1H\}$ NMR ($CDCl_3$; δ, ppm): 72.3 (s). ^{19}F NMR ($CDCl_3$; δ, ppm): –78.4 (s).

IR (ν, cm^{-1}): 1788 m, 1533 w, 1460 m, 1400 m, 1382 m, 1318 w, 1265 s,1219 m, 1146 s, 1028 s, 996 m, 920 m, 856 w, 833 m, 801 s, 767 s, 752 m, 719 w, 636 vs, 574 vs.

Synthesis of [(DDP)Cl](OTf) (III). A solution of trimethylsilyl triflate (0.22 g, 1.0 mmol) in dichloromethane (10 mL) was added at 0°C to a solution of cyclohexane-annulated 1,4-dichloro-3a,6a-diaza-1,4-diphosphapentalene (**I**, [6]) (0.32 g, 1.0 mmol) in dichloromethane (15 mL). The reaction mixture was kept for 1 h at room temperature, the volatile components were removed in vacuum, and the solid residue was recrystallized from toluene. The yield of **III** was 0.31 g (73%).

For $C_{13}H_{16}ClF_3N_2O_3P_2S$ (M = 434.74)

Anal. calcd., %	C, 35.92	H, 3.71	N, 6.44	P, 14.25
Found, %	C, 34.87	H, 3.75	N, 6.40	P, 14.19

^{1}H NMR ($CDCl_3$; δ, ppm): 3.05–1.43 (m., 16 H, cHex). $^{31}P\{^1H\}$ NMR ($CDCl_3$; 223 K; δ, ppm): 228.4 (d, $^3J_{P,P}$ = 20 Hz), 98.3 (d, $^3J_{P,P}$ = 20 Hz). ^{19}F NMR ($CDCl_3$; δ, ppm): –78.0 (s).

IR (ν, cm^{-1}): 1626 m, 1251 br.m, 1148 br.m, 1024 s, 910 m, 854 m, 816 w, 800 m, 726 m, 636 s, 590 w, 571 m, 548 m, 515 s, 493 w, 479 m, 462 s.

Synthesis of [(DDP*)Cl](OTf) (V). A solution of trimethylsilyl triflate (0.44 g, 2.0 mmol) in dichloromethane (10 mL) was added at 0°C to a solution of tetrahydronaphthalene-annulated 1,4-dichloro-3a,6a-diaza-1,4-diphosphapentalene (**IV**, [1]) (0.42 g, 1.0 mmol) in dichloromethane (15 mL). The reaction mixture was kept for 1 h at room temperature and concentrated. The precipitated yellow crystals were recrystallized from dichloromethane. The yield of **V** was 0.36 g (69%).

For $C_{21}H_{16}ClF_3N_2O_3P_2S$ (M = 530.82)

Anal. calcd., %	C, 47.52	H, 3.04	N, 5.28	P, 11.67
Found, %	C, 47.49	H, 3.08	N, 5.32	P, 11.63

^{1}H NMR ($CDCl_3$; δ, ppm): 8.5–7.0 (m, 8H, aryl), 3.0–1.8 (m, 8H, $-CH_2-$). $^{31}P\{^1H\}$ NMR ($CDCl_3$; δ, ppm): 230.0 (br.s), 110.0 (br.s). ^{19}F NMR ($CDCl_3$; δ, ppm): –81.0 (s).

IR (ν, cm^{-1}): 1604 m, 1335 w, 1300 w, 1275 m, 1238 m, 1159 m, 1087 m, 1027 s, 903 w, 887 w, 805 m, 775 m, 764 m, 726 m, 693 w, 673 w, 653 w, 635 s, 608 w, 573 w, 540 w, 518 m, 493 m, 458 w.

The ^{1}H, ^{31}P, and ^{19}F NMR spectra were recorded on a Bruker AV400 (400 MHz) spectrometer. UV-Vis spectra were measured on a Perkin-Elmer Lambda UV–Vis instrument. The IR spectra of the products as mineral oil mulls were measured on an FSM 1201 FTIR spectrometer in the range from 4000 to 400 cm^{-1}. The elemental analysis was carried out using an Elementar vario EL cube elemental analyzer for C, H, and N determination. Phosphorus was quantified by the gravimetric method using the dry residue resulting from pyrolysis. The redox potentials of compounds **II**, **III**, DMAP, and dimethyl(1*H*-pyridin-4-yliden)ammonium triflate (c = 5 mM) were measured by cyclic voltammetry (CV) in a standard three-electrode cell under argon using a Corrtest CS300 potentiostat/galvanostat (China). A glassy carbon working electrode (1 mm), a platinum wire auxiliary electrode, and an Ag/AgCl/NaCl reference electrode were used. The potential sweep rate was 100 mV/s. The supporting electrolyte was 0.1 M nBu$_4$NPF$_6$ (≥99%, Sigma-Aldrich). Compensation for the ohmic voltage loss was performed by the positive feedback method, with the numerical value of resistance being determined by the electrochemical circuit interruption method.

X-ray diffraction study of II, III, and V. Crystallographic data were collected on Bruker D8 Quest (for **II** and **III**) and Agilent Xcalibur E (for **V**) automated single-crystal diffractometers (MoK_α radiation, φ- and ω-scan modes, λ = 0.71073 Å). The X-ray diffraction data collection, the initial reflection indexing, and the refinement of unit cell parameters were carried out using APEX3 [7] (for **II** and **III**) and CrysAlisPro (for **V**) software [8]. The experimental sets of intensities were integrated using the SAINT [9, 10] (for **II** and **III**) and CrysAlisPro (for **V**) software [8]. The structures were solved by direct methods using the dual-space algorithm in the SHELXT program [11]. The non-hydrogen atoms were refined by the full-matrix least-squares method on F^2_{hkl} in the anisotropic approximation using the SHELXTL program package [12, 13]. The absorption corrections were applied using the SADABS [14] and SCALE3 ABSPACK [15] software for **II**, **III**, and **V**, respectively. The hydrogen atoms were placed into geometrically calculated positions and refined in the riding model (U_{iso}(H) = 1.5U_{equib}(C) for CH_3 groups; U_{iso}(H) = 1.2U_{equiv}(C) for the other groups). The Cy moieties in complexes **II** and **V** and one triflate anion in **II** were disordered over two and three positions, respectively. The main crystallographic characteristics and refinement parame-

Table 1. Crystallographic data and structure refinement details for **II**, **III**, and **V**

Parameters	Value		
	II	**III**	**V**
Molecular formula	$C_{28}H_{36}F_6N_6O_6P_2S_2$	$C_{13}H_{16}N_2O_3F_3P_2SCl$	$C_{21}H_{16}N_2O_3F_3P_2SCl$
M	792.69	434.73	530.81
Temperature, K	200(2)	100(2)	100(2)
System	Monoclinic	Monoclinic	Monoclinic
Space group	$C2/c$	$P2_1/c$	$P2_1/c$
a, Å	20.3575(7)	12.1776(4)	8.3692(5)
b, Å	18.3048(6)	14.9308(5)	21.0036(11)
c, Å	19.3626(7)	9.5362(3)	13.1038(7)
α, deg	90	90	90
β, deg	104.411(1)	92.860(1)	105.481(6)
γ, deg	90	90	90
V, Å^{-3}	6988.2(4)	1731.72(10)	2219.9(2)
Z	8	4	4
ρ, mg m^{-3}	1.507	1.667	1.588
μ, mm^{-1}	0.326	0.573	0.464
F(000)	3280	888	1080
Crystal size, mm	0.43 × 0.30 × 0.12	0.44 × 0.19 × 0.15	0.36 × 0.21 × 0.13
Data collection range of θ, deg	2.17–26.73	2.54–30.12	3.19–30.00
Ranges of reflection indices	$-25 \le h \le 25$, $-23 \le k \le 23$, $-24 \le l \le 24$	$-17 \le h \le 17$, $-21 \le k \le 21$, $-13 \le l \le 13$	$-11 \le h \le 10$, $-25 \le k \le 29$, $-18 \le l \le 17$
Number of measured reflections	53162	39494	12888
Number of unique reflections	7423	5080	6466
Reflections with $I > 2\sigma(I)$	6154	4240	4600
R_{int}	0.0281	0.0297	0.0419
Number of refinement parameters	520	234	298
GOOF (F^2)	1.005	1.037	1.017
R_1, wR_2 ($I > 2\sigma(I)$)	0.0396, 0.1124	0.0486, 0.1082	0.0536, 0.1204
R_1, wR_2 (on F^2 for all reflections)	0.0506, 0.1211	0.0616, 0.1147	0.0860, 0.1313
Residual electron density (ρ_{min}/ρ_{max}), e Å^{-3}	0.510/–0.378	0.968/–0.985	0.736/–0.538

ters for **II**, **III**, and **V** are summarized in Table 1 and the bond lengths and bond angles are given in Table 2.

The crystallographic data were deposited with the Cambridge Crystallographic Data Centre (CCDC no. 2182881 (**II**), 2182882 (**III**), and 2182883 (**V**); deposit@ccdc.cam.ac.uk or http://www.ccdc.cam.ac.uk).

RESULTS AND DISCUSSION

A deficiency of electron density in the heteropentalene skeleton can be generated by replacing the covalently bound halogen atom in DDP dichloride by a triflate anion. For this purpose, the appropriate diazadiphosphapentalene dichloride is treated with trimethylsilyl triflate.

^{31}P NMR analysis of the reaction mixture containing cyclohexane-annulated 1,4-dichloro-3a,6a-diaza-1,4-diphosphapentalene (**I**) and TMSOTf (1 : 2) in dichloromethane showed the absence of any signals at room temperature. Meanwhile, the addition of 2 equiv. of DMAP to this reaction mixture gave rise to a singlet at 72.3 ppm. The removal of the solvent and volatile products in vacuum gave a high yield of complex salt **II** (Scheme 3), which was characterized by X-ray diffraction analysis.

Table 2. Selected bond lengths (Å) and bond angles (deg) in complexes **II**, **III**, and **V**

Bond	*d*, Å	Angle	ω, deg
		II	
P(1)–N(1)	1.703(2)	N(1)P(1)C(1)	87.80(8)
P(1)–N(3)	1.815(2)	N(1)P(1)N(3)	105.03(7)
P(1)–C(1)	1.800(2)	C(1)P(1)N(3)	99.67(8)
C(1)–C(2)	1.349(3)		
N(1)–N(2)	1.425(2)	P(1)N(1)N(2)	115.35(11)
N(1)–C(8)	1.382(2)	P(2)N(2)N(1)	115.02(11)
N(2)–C(2)	1.386(2)		
C(7)–C(8)	1.352(3)	N(2) P(2)C(7)	88.10(8)
C(7)–P(2)	1.791(2)	N(2)P(2)N(5)	104.36(7)
N(2)–P(2)	1.700(2)	C(7)P(2)N(5)	100.78(8)
N(5)–P(2)	1.813(2)		
		III	
Cl(1)–P(1)	2.080(1)	N(1)P(1)C(1)	86.90(10)
P(1)–N(1)	1.775(2)	N(1)P(1)Cl(1)	97.33(7)
P(1)–C(1)	1.811(2)	C(1)P(1)Cl(1)	98.51(8)
P(2)–N(2)	1.685(3)		
P(2) –C(7)	1.739(3)	N(2)P(2)C(7)	89.28(10)
N(1)–C(8)	1.351(3)		
N(1)–N(2)	1.363(3)	N(2)N(1)P(1)	114.88(15)
N(2)–C(2)	1.414(3)	N(1)N(2)P(2)	114.50(15)
C(1)–C(2)	1.342(3)		
C(7)–C(8)	1.392(3)		
		V	
Cl(1)–P(1)	2.096(1)	N(1)P(1)C(1)	87.62(10)
P(1)–N(1)	1.771(2)	N(1)P(1)Cl(1)	101.24(7)
P(1)–C(1)	1.798(2)	C(1)P(1)Cl(1)	98.75(8)
P(2)–N(2)	1.691(2)		
P(2)–C(7)	1.727(2)	N(2)P(2)C(7)	89.47(10)
N(1)–C(8)	1.352(3)		
N(1)–N(2)	1.385(3)	N(2)N(1)P(1)	113.88(14)
N(2)–C(2)	1.411(3)	N(1)N(2)P(2)	115.05(14)
C(1)–C(2)	1.347(3)		
C(7)–C(8)	1.397(3)		

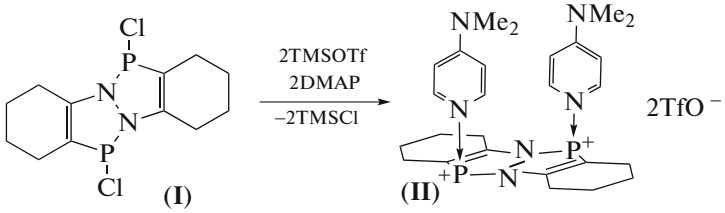

Scheme 3.

The molecular and crystal structures of the dicationic part of complex **II** are shown in Figs. 1 and 2.

The asymmetric part of the unit cell of **II** contains the $[DDP(DMAP)_2]^{2+}$ dication (Fig. 1) and two tri-

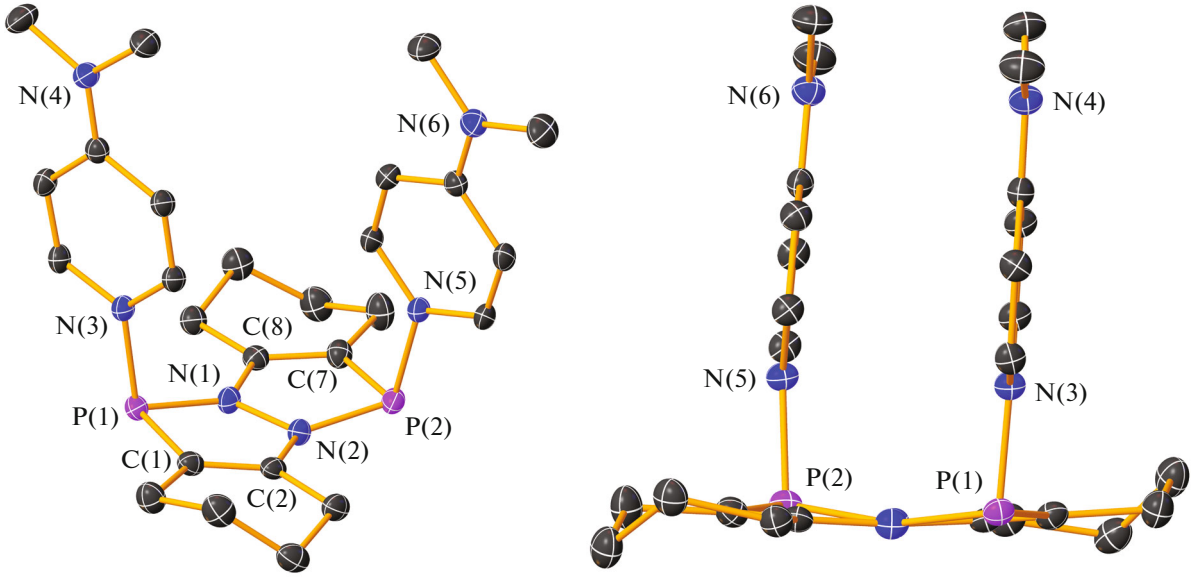

Fig. 1. Molecular structure of the cationic part of complex **II** with thermal ellipsoids drawn at 30% probability level in two projections. Hydrogen atoms are omitted for clarity.

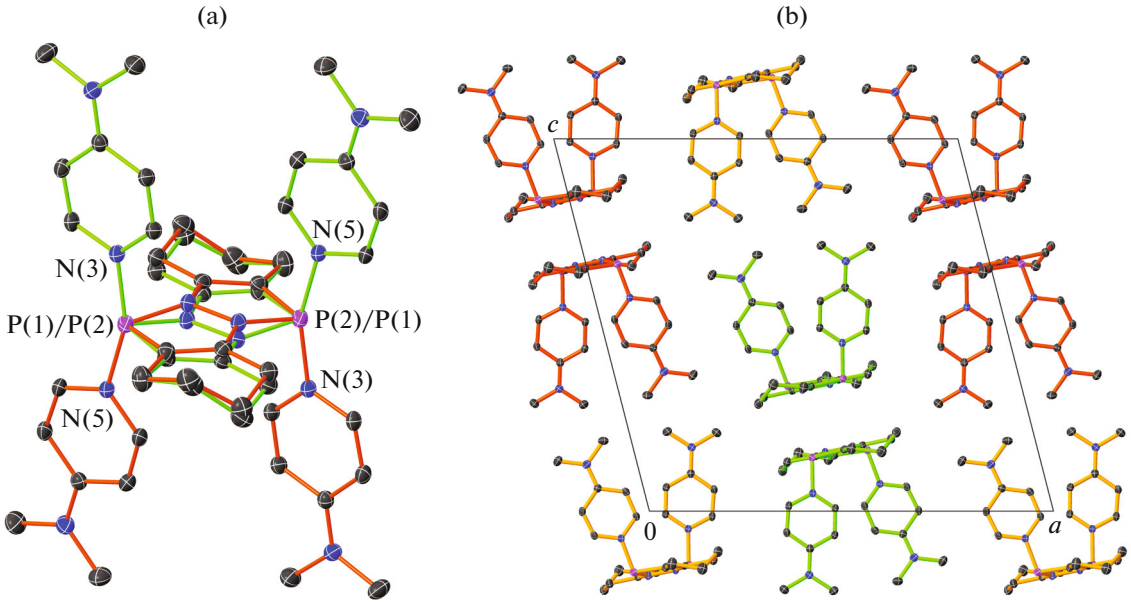

Fig. 2. (a) Superposition of two stereoisomeric forms of $[DDP(DMAP)_2]^2$ **II**; (b) fragment of packing of $[DDP(DMAP)_2]^{2+}$ molecules in the crystal of **II**.

flate anions. The crystals of **II** incorporate two enantiomers of the $[DDP(DMAP)_2]^{2+}$ dication, which differ by the positions of 4-dimethylaminopyridine substituents relative to the DDP plane (Fig. 2a). The five-membered heterocycles have a nearly planar structure. The average deviations of atoms from the N(1)N(2)P(1)C(2)C(1) and N(2)N(1)P(2)C(8)C(7) planes do not exceed 0.029 and 0.049 Å, respectively. The sum of the bond angles at the heteropentalene nitrogen atoms is 359.09° for N(1) and 358.41° for N(2). The DMAP molecules are coordinated to the P(1) and P(2) atoms on one side of the DDP skeleton, thus forming angles of 105.26° and 104.25°, respectively, with the planes of five-membered heterocycles. The coordination bond lengths (P(1)–N(3), 1.815(2); and P(2)–N(5), 1.813(2) Å) are close to the sum of the covalent radii of these elements (1.82 Å) [16]. It is noteworthy that the DMAP ligands are planar, indi-

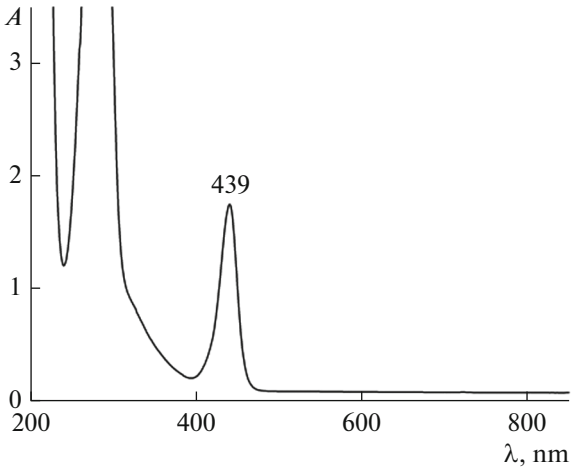

Fig. 3. UV-Vis spectrum of **II** in CH_2Cl_2.

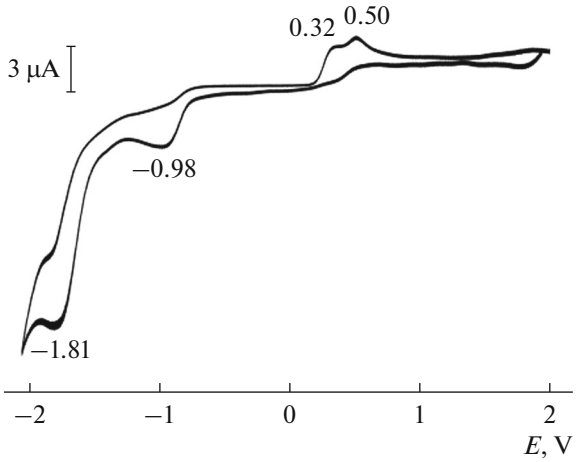

Fig. 4. CV of compound **II** in CH_2Cl_2/Bu_4NPF_6 (0.1 M), potential sweep rate of 100 mV/s, vs. Ag/AgCl.

cating sp^2-hybridization of the Me_2N nitrogen atoms and a significant positive charge transfer from the phosphorus atoms to these groups. It is also of interest that DMAP molecules are located in parallel planes.

Analysis of the crystal packing of **II** shows that each stereoisomer of $[DDP(DMAP)_2]^{2+}$ is arranged in 1D chains along the *c* axis (Fig. 2b). The chains of the isomers alternate along the *a* axis. Note that in the chains extended along the *c* axis, the $[DDP(DMAP)_2]^{2+}$ molecules are aligned in pairs, facing each other with heteropentalene bases located at a distance of approximately 3.5 Å.

4-Dimethylaminopyridine is known for its donor properties, which are utilized, in particular, for stabilization of phosphorus-centered cations, for example, $[(DMAP)PPh_2]^+$ [17], $[(DMAP)\text{-}(PBu^t)_3\text{-}Me]^+$ [18], and $[P_3N_3(DMAP)_6]^{6+}$ [19].

The crystals of complex **II** are colorless, but solutions exhibit all signs of solvatochromism. In dichloromethane, a band at 439 nm appears in addition to the intense band at 280 nm corresponding to the complex (Fig. 3). The new band may be assigned to free diazadiphosphapentalene (438 nm/THF [5]), which is formed in the solution upon the equilibrium disproportionation of **II** (Scheme 4).

$$2[(DDP)(DMAP)_2](OTf)_2 \rightleftharpoons DDP + [(DDP)(DMAP)_4](OTf)_4$$

(II)

Scheme 4.

The UV-Vis spectrum of free 4-dimethylaminopyridine shows an intense band at 258 nm (CH_2Cl_2) [20]; no such band is present in the solution of **II**.

Previously, we observed similar disproportionation processes in solutions of DDP dichlorides in donor solvents [21]. A cyclic voltammetric study of solutions of **II** showed the presence of oxidation peak potentials of 0.32 and 0.50 V; this confirms the presence of DDP molecules, which are easily oxidized (Fig. 4). The potentials of the first and second oxidation peaks of free cyclohexane-annulated DDP in methylene chloride are 0.15 and 0.39 V [4]. 4-Dimethylaminopyridine is oxidized at a higher potential under the same conditions (1.36 V, Fig. 5*a*). The reduction of dimethyl(1*H*-pyridin-4-ylidene)ammonium triflate occurs at a relatively high potential of −1.9 V (Fig. 5*b*).

It is important to note that dilute solutions of compound **II** in ether solvents (THF) are unstable, apparently, due to the competing replacement of the DMAP ligand by solvent molecules, followed by transformations of the substitution products. Upon dilution of solutions of **II** in THF down to concentration of ~1 mg/mL, the complex is destroyed to quantitatively give dimethyl(1*H*-pyridin-4-ylidene)ammonium triflate $[(Me_2NC_6H_4NH)^+(CF_3SO_3)^-]$ and an unidentified resinous product. The dissolution of complex **II** in deuterated tetrahydrofuran furnishes a crystalline precipitate, which was also identified as dimethyl(1*H*-pyridin-4-ylidene)ammonium triflate (but not dimethyl(1D-pyridin-4-ylidene)ammonium triflate, as evidenced by the IR spectrum). This indicates that the cyclohexyl moieties of the complex serve as the sources of protons (Scheme 5). The molecular structure of dimethyl(1*H*-pyridin-4-ylidene)ammonium triflate was studied by X-ray diffraction and was completely in line with the structure studied previously [22].

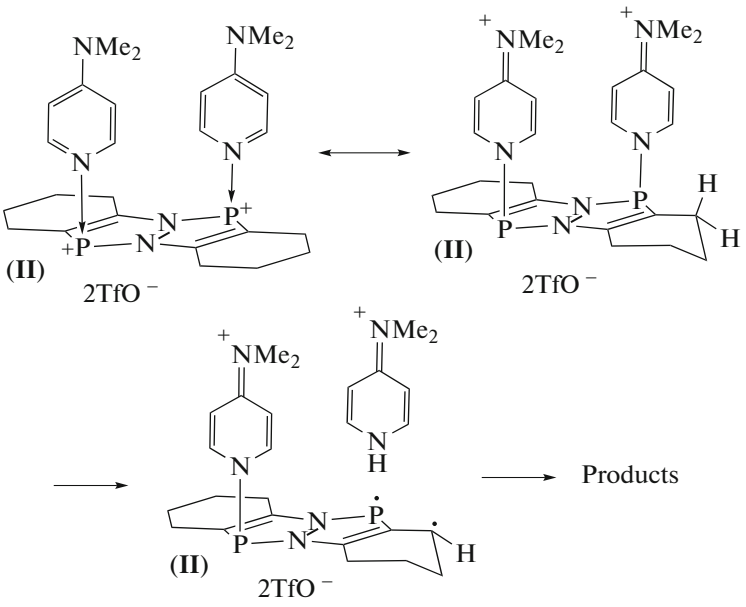

Scheme 5.

Note that the use of unsubstituted pyridine instead of DMAP in the reaction with TMSOTf does not give a stable complex.

The ^{31}P NMR spectra of complex **II** at room temperature in CD_2Cl_2 or $CDCl_3$ exhibit broad singlets, which implies dynamic behavior in solution. Using DFT/B3LYP calculations in the 6-31G(d) basis set, we optimized the geometry of the possible isomeric dications containing DMAP ligands in different positions (Fig. 6). The 1,4-*cis* (a) and 1,4-*trans* (b) isomers have fairly similar total energies, differing by 2.2 kcal/mol. However, the most stable 1,4-isomer (b) is not experimentally observed in the crystalline state, apparently due to the less favorable packing compared to 1,4-*cis*-isomer. The 1,1-isomers (c, d) have higher total energies.

A detailed study of the DDP dichloride–TMSOTf system demonstrated that at their 1 : 1 ratio, the reactions give single compounds resulting from the replacement of one chlorine atom by a triflate group. We performed these reactions for diazadiphosphapentalene dichlorides **I** and **IV** (Scheme 6).

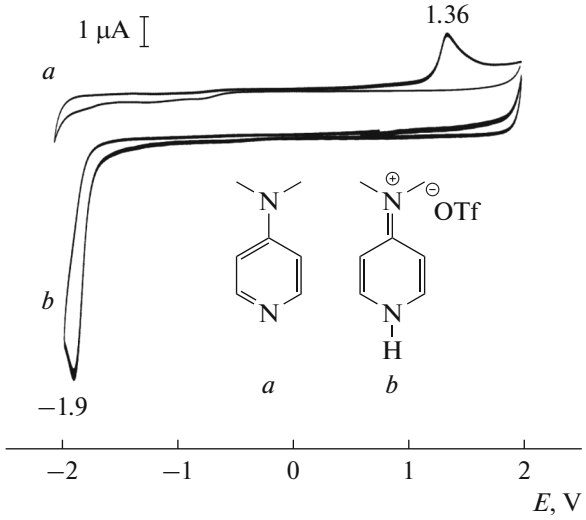

Fig. 5. Cyclic voltammogram of (a) 4-dimethylaminopyridine and (b) dimethyl(1*H*-pyridin-4-ylidene)ammonium triflate in CH_2Cl_2/Bu_4NPF_6 (0.1 M), potential sweep rate of 100 mV/s, vs. Ag/AgCl.

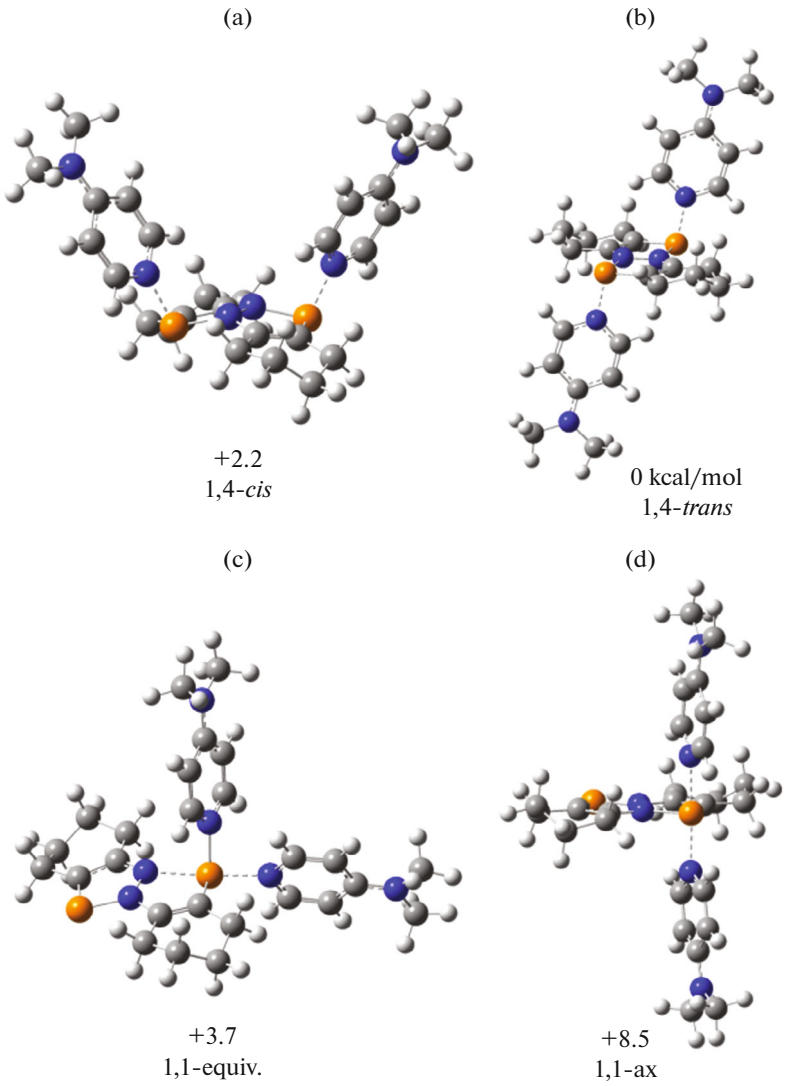

Fig. 6. DFT/B3LYP/6-31G(d)-optimized structures and relative total energies (kcal/mol) of isomeric $[DDP(DMAP)_2]^{2+}$ dications.

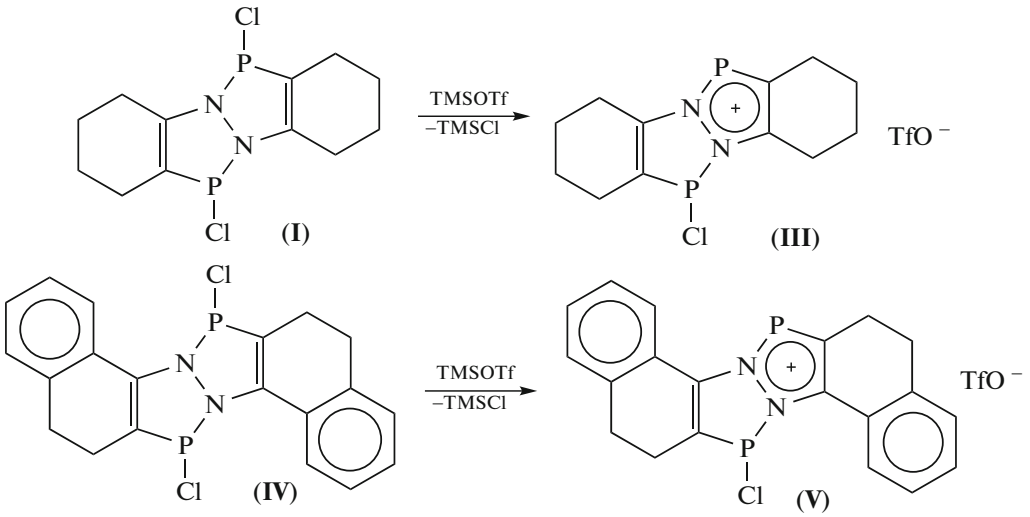

Scheme 6.

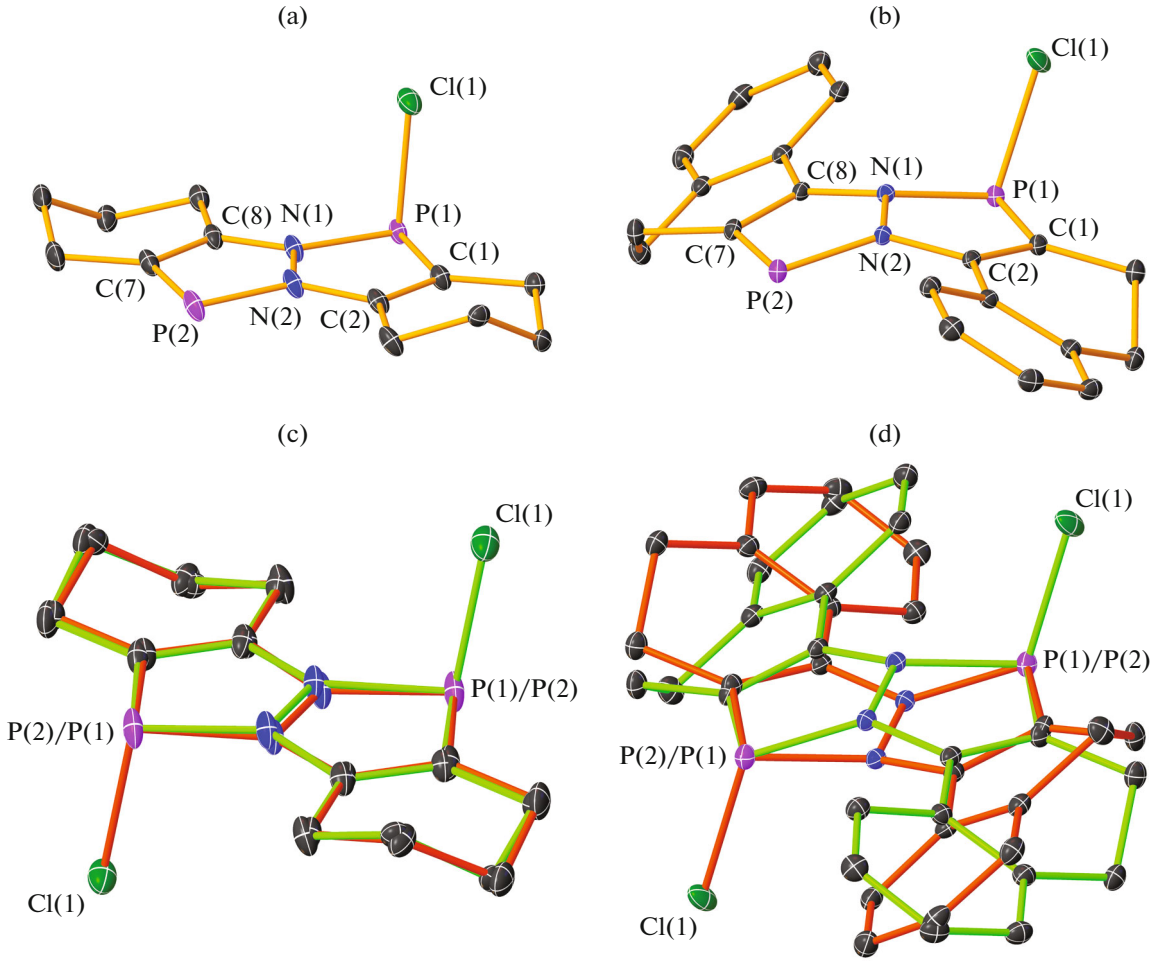

Fig. 7. Molecular structures of the cationic moieties of complexes (a) **III** and (b) **V** with thermal ellipsoids drawn at 30% probability level (hydrogen atoms are omitted for clarity); superposition of two stereoisomers of $[ClDDP]^+$ complexes (c) **III** and (d) **V**.

The single crystals of compounds **III** and **V** were obtained by recrystallization from toluene and dichloromethane, respectively. The molecular structures of the cationic parts of complexes **III** and **V** are shown in Figs. 7a, 7b.

According to X-ray diffraction data, complexes **III** and **V** consist of separated $[ClDDP]^+$ and $[TfO]^-$ ions. The crystals of **III** and **V** (like **II**) contain pairs of geometric isomers of $[ClDDP]^+$ (Figs. 7c, 7d). Despite the similarity of structural parameters, the structures of DDP skeletons in complexes **III** and **V** differ (Figs. 7a, 7b).The geometry of the DDP skeleton of **III** is nearly planar, with the average atom deviation from the plane being 0.02 Å. At the same time, the molecule of **V** is bent along the N–N bond, which is evidenced by the values of torsional angles: the P(1)N(1)N(2)P(2) angle of 157.5(1)° and the C(2)N(2)N(1)C(8) angle of 165.1(2)° (for **III**, these values are close to 180°, being 176.1(1)° and 175.7(2)°).

The five-membered heterocycles containing two- and three-coordinate phosphorus atoms differ in structural parameters. The bond lengths in the five-membered heterocycles that contain a two-coordinate phosphorus atom correspond to those in aromatic diazaphospholes [23]. In particular, multiple (1.5-order) C(7)–C(8) carbon–carbon bonds (1.397(3) Å (**V**) and 1.392(3) Å (**III**)) are markedly longer than the C(1)–C(2) bonds in the neighboring rings (1.347(3) Å (**V**) and 1.342(3) (**III**)), which are typical of alkenes. The P(1)–Cl(1) bonds (2.080(1) Å (**III**) and 2.096(1) Å (**V**)) are somewhat shortened compared to those in the starting dichloride **I** (2.1762(6)), which corresponds to the sum of covalent radii of P and Cl (2.10 Å) [16].

In the crystal of **III**, the triflate anions form short P···O contacts with two-coordinate (P(2)···O(1), 2.881(2) Å) and three-coordinate (P(1)···O(2), 2.874(2) Å) phosphorus atoms, thus forming chains of the complexes along the *a* axis (Fig. 8a). Similar P···O contacts in the crystal of **V** with 2.886(2) Å

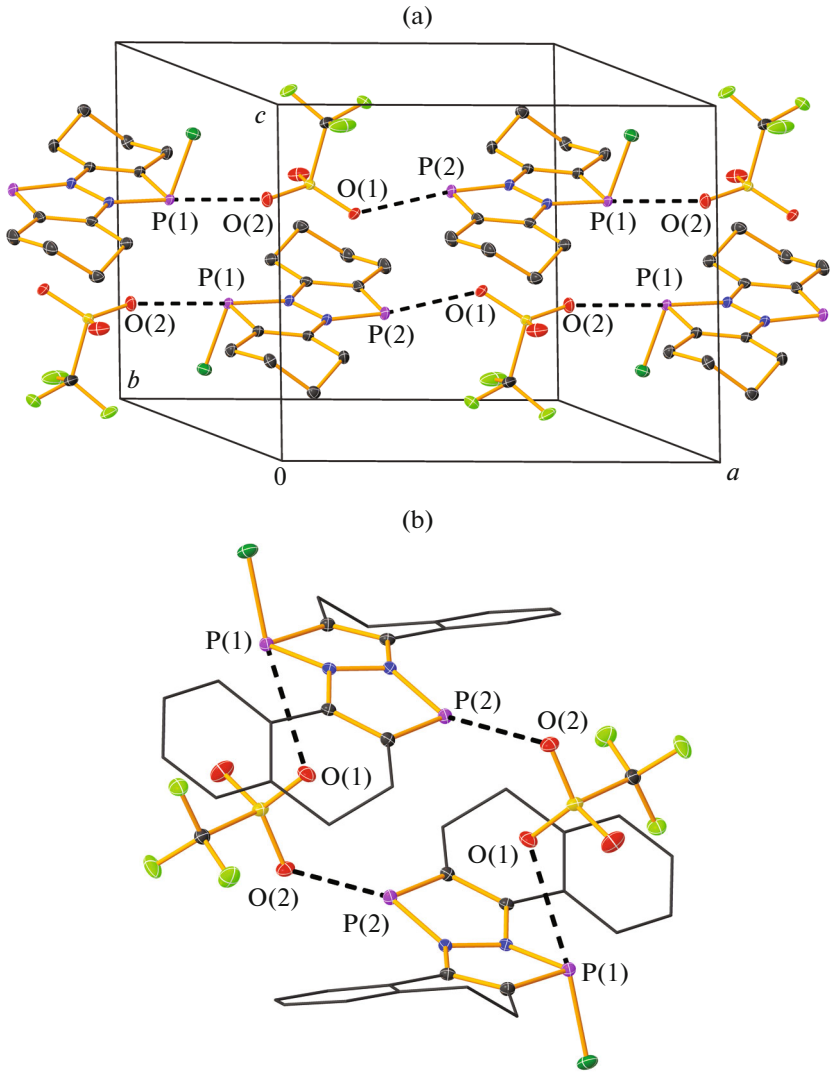

Fig. 8. Shortened P···O contacts in (a) **III** and (b) **V**.

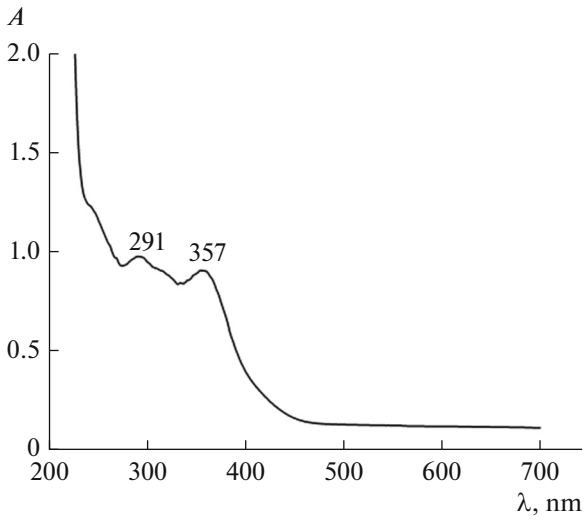

Fig. 9. UV-Vis spectrum of **III** in CH_2Cl_2.

(P(1)···O(1)) and 2.958(2) Å (P(2)···O(2)) distances give rise to dimeric motif of complex **V** (Fig. 8b).

Interestingly, in the crystal structure of complex **II**, no P···O contacts are present, which is evidently attributable to a significant transfer of the positive charge towards the nitrogen atoms of the Me_2N groups. Meanwhile, structure **II** has shortened O···H contacts involving hydrogen atoms of the pyridyl moiety (~2.2 Å).

The behavior of compound **III** in solution was studied by NMR spectroscopy, cyclic voltammetry (CV), and UV-Vis spectroscopy. At room temperature, the ^{31}P NMR spectrum in chloroform consists of two very broad singlets (230.1 and 100.5 ppm). As the temperature is lowered to 223 K, they are converted to two doublets (228.4 and 98.3 ppm) with the spin–spin coupling constant $^3J_{P,P} = 20$ Hz. In dichloromethane, toluene, or THF, the ^{31}P NMR signal is not mani-

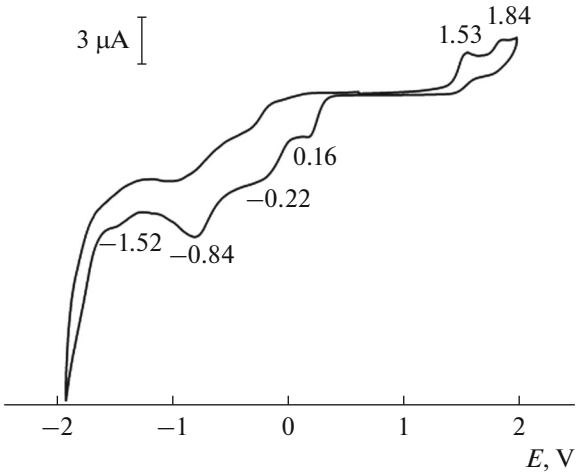

Fig. 10. Cyclic voltammogram of compound **III** in CH_2Cl_2/Bu_4NPF_6 (0.1 M), potential sweep rate of 100 mV/s, vs. Ag/AgCl.

fested at 295 K, which is attributable to the associative dynamic behavior of compound **III** in solution. The UV-Vis spectra (Fig. 9) exhibit absorption bands at 357 and 291 nm, that is, in the region typical of diazadiphosphapentalene dichlorides [21].

Compound **III** is both reduced and oxidized markedly more easily than the stabilized dication **II**. The reduction peak is observed at 0.16 V (versus Ag/AgCl, Fig. 10). The oxidation peak potentials of **III** are 1.53 and 1.84 V, whereas compound **II** is not oxidized in dichloromethane under experimental conditions (Fig. 4).

It is known that boron-containing Lewis acids, in particular BCl_3, can actively add halide anions to form stable complex anions. We studied the reaction of DDP dichloride (**I**) with boron trichloride and found that the mixture of these reactants exists in equilibrium and does not produce single compounds. Nevertheless, mention should be made of the ^{31}P NMR spectra in which interesting trends can be followed. The ^{31}P NMR spectrum of the starting dichloride **I** (106.0 ppm, singlet) shifts downfield (155.5 ppm) upon the addition of 2 equiv. of BCl_3 in toluene. In addition, cooling of the sample from 293 to 233 K is accompanied by considerable signal broadening and decrease in signal intensity. This implies that the point of coalescence is below the experimental temperature (233 K). The replacement of the solvent (toluene) by electron-donor tetrahydrofuran leads to the starting dichloride **I** and BCl_3·THF.

Thus, we have shown that in the absence of coordinating agents, only one chlorine atom in 1,4-dichloro-3a,6a-diaza-1,4-diphosphapentalenes is replaced by triflate anion to give cationic type DDP, that is, $[ClDDP]^+[TfO]^-$. Substitution of triflate anions for two chlorine atoms is possible only if the DDP dication is stabilized by donor molecules, in particular, 4-dimethylaminopyridine. Then the reaction gives the complex salt $[DDP(DMAP)_2]^{2+}[(CF_3SO_3)^-]_2$ (**II**). In dilute solutions, compound **II** decomposes to give dimethyl(1*H*-pyridin-4-ylidene)ammonium triflate and unidentified phosphorus-containing products.

FUNDING

This study was supported by the Russian Science Foundation (project no. 19-13-00400-P) and was performed using equipment of the Center for Collective Use, Analytical Center of the Razuvaev Institute of Organometallic Chemistry, Russian Academy of Sciences, under the grant "Provision of the Development of the Material and Engineering Infrastructure of the Centers for Collective Use of Research Equipment" (Contract 13.TsKP.21.0017 (075-15-2021-670), RF 2296.61321X0017).

CONFLICT OF INTEREST

The authors declare that they have no conflicts of interest.

REFERENCES

1. Kornev, A.N., Panova, Y.S., Sushev, V.V., et al., *Inorg. Chem.*, 2019, vol. 58, p. 16144.
2. Kornev, A.N., Panova, Y.S., and Sushev, V.V., *Phosphorus, Sulfur, Silicon, Relat. Elem.*, 2020, vol. 195, p. 905.
3. Kornev, A.N., Panova, Y.S., Sushev, V.V., et al., *Russ. J. Coord. Chem.*, 2020, vol. 46, no. 2, p. 98. https://doi.org/10.1134/S1070328420020050
4. Panova, Yu., Khristolyubova, A., Zolotareva, N., et al., *Dalton Trans.*, 2021, vol. 50, p. 5890.
5. Kornev, A.N., Sushev, V.V., Panova, Yu.S., et al., *Inorg. Chem.*, 2014, vol. 53, p. 3243.
6. Kornev, A.N., Gorak, O.Y., Lukoyanova, O.V., et al., *Z. Anorg. Allg. Chem.*, 2012, vol. 638, nos. 7–8, p. 1173.
7. *APEX3. Bruker Molecular Analysis Research Tool. Version 2016.9*, Madison: Bruker AXS Inc., 2016.
8. *Data Collection, Reduction and Correction Program. CrysAlisPro 1.171.38.46. Software Package*, Rigaku OD, 2015.
9. *SAINT Data Reduction and Correction Program, Version 8.37A*, Madison: Bruker AXS Inc., 2012.
10. Krause, L., Herbst-Irmer, R., Sheldrick, G.M., and Stalke, D., *J. Appl. Crystallogr.*, 2015, vol. 48, p. 3.
11. Sheldrick, G.M., *Acta Crystallogr., Sect. A: Found. Adv.*, 2015, vol. 71, p. 3.
12. Sheldrick, G.M., *Acta Crystallogr., Sect. C: Struct. Chem.*, 2015, vol. 71, p. 3.
13. Sheldrick, G.M., *SHELXTL. Version 6.14. Structure Determination Software Suite*, Madison: Bruker AXS, 2003.
14. Sheldrick, G.M., *SADABS. Version 2016/2. Bruker/Siemens Area Detector Absorption Correction Program*, Madison: Bruker AXS Inc., 2016.

15. *SCALE3 ABSPACK: Empirical Absorption Correction. CrysAlisPro 1.171.38.46. Software Package*, Rigaku OD, 2015.

16. Pyykkö, P. and Atsumi, M., *Chem.-Eur. J.*, 2009, vol. 15, no. 1, p. 186.

17. Burford, N., Losier, P., Phillips, A.D., et al., *Inorg. Chem.*, 2003, vol. 42, p. 1087.

18. Robertson, A.P.M., Dyker, C.A., Gray, P.A., et al., *J. Am. Chem. Soc.*, 2014, vol. 136, p. 14941.

19. Boomishankar, R., Ledger, J., Guilbaud, J.-B., et al., *Chem. Commun.*, 2007, p. 5152.

20. Huang, C.H., Wen, M., Wang, C.Y., et al., *Dalton Trans.*, 2017, vol. 4, no. 5, p. 1413.

21. Panova, Yu.S., Khristolyubova, A.V., Sushev, V.V., et al., *Russ. Chem. Bull., Int. Ed.*, 2021, vol. 70, no. 10, p. 1973. https://link.springer.com/article/10.1007/s11172-021-3305-1

22. Bock, H., Nather, C., John, A., et al., *CSD Communication (Private Communication)*, 2007, CCDC 228884.

23. Nyulaszi, L., Veszpremi, T., Reffy, J., et al., *J. Am. Chem. Soc.*, 1992, vol. 114, no. 23, p. 9080.

Translated by Z. Svitanko